Case Report

Synchronous tri-cavitary biphasic malignant mesothelioma in a dog presenting with dyspnea

Nawarus Prapaiwan[1*] Poonavit Pichayapaiboon[2] Tawewan Issarankura Na Ayudhaya[3]

Onrampha Tanglakmankhong[4]

Abstract

Malignant mesothelioma is an uncommon tumor that has a challenging diagnosis and a tendency for late diagnosis. A 7-year-old intact male dog presented with respiratory distress. Thoracic radiography revealed pleural effusion and bone reactions at multiple ribs. A computerized tomography scan with rib biopsy was suggested as a diagnosis plan. Unfortunately, the dog died. Gross pathological findings demonstrated multifocal to coalescing, pinkish-white firm masses scattered over the parietal pleural surface, extended to the serosa of the diaphragm and the pericardium, making them adhere to each other and causing the coalescence of a white irregular mass at the diaphragm. Multiple white to pink nodules were also noted at the intercostal muscle, mediastinum, and peritoneum. The histopathologic findings indicated a diffuse nodular structure of neoplasm in the pleura, mediastinum, pericardium, peritoneum, and lungs. The nodules were mainly composed of neoplastic epithelioid cells mixed with a minor component of atypical spindle-shaped cells. A biphasic malignant mesothelioma was considered according to gross appearance, location of lesions, and histopathological findings. The histopathological characteristics of this tumor were confirmed by immunohistochemical staining of vimentin, cytokeratin, and desmin. This report describes the pathomorphological, histopathological, and immunohistochemical features of tri-cavitary biphasic malignant mesothelioma in a dog.

Keywords: biphasic malignant mesothelioma, dog, dyspnea, immunohistochemistry

[1]*Department of Clinical Sciences and Public Health, Faculty of Veterinary Science, Mahidol University, Nakhon Pathom 73170, Thailand*

[2]*Prasu-Arthorn Animal Hospital, Faculty of Veterinary Science, Mahidol University, Nakhon Pathom, 73170, Thailand*

[3]*Department of Preclinic and Applied animal Science, Faculty of Veterinary Science, Mahidol University, Nakhon Pathom, 73170, Thailand*

[4]*Veterinary Diagnostic Center, Faculty of Veterinary Science, Mahidol University, Nakhon Pathom, 73170, Thailand*

****Correspondence****: nawarus.pra@mahidol.edu* (N. Prapaiwan)

Received: August 22, 2023

Accepted: September 18, 2023

Introduction

Mesothelioma is a mesodermal neoplasm originating from the cells of a serosal surface, such as the pericardium, pleural cavity, peritoneum, and tunica vaginalis (Jeff and Kurt, 2016). The development of mesothelioma may be significantly influenced by exposure to asbestos and silica (Lawrence *et al.*, 1983; Laura, 2020). Although canine mesothelioma is generally regarded as a rare case, these tumors are usually malignant (Francisco *et al.*, 2016). The prevalence of this tumor has been estimated to be 1 in 1000 dogs (Laura, 2020). The pleura and pericardium are commonly affected in dogs, followed by the peritoneum. In bi-cavitary mesothelioma, sites include pericardium and pleura, pleura and peritoneum, and peritoneum along with pericardium. The incidence of tri-cavitary mesothelioma is relatively low compared to other affected locations, with an occurrence rate of 1.7% (Lajoinie *et al.*, 2022). Mesothelioma presents as a diffuse nodular mass covering the surfaces of the body cavity with extensive effusion that could result from the tumor itself or secondary development to a lymphatic tract obstruction. Therefore, the most common presenting signs are dyspnea from pleural effusion or a distended abdomen from peritoneal effusion (Laura, 2020). Moreover, dogs with pericardial or heart-based mesothelioma could suffer from cardiac tamponade or heart failure (Cobb and Brownlie, 1992). Distant metastases, though infrequent, have been observed in regional lymph nodes and bone marrow in certain cases (Smith and Hill, 1989). Mesotheliomas can be classified into three histologic subtypes including (i) Epithelioid mesothelioma, which resembles an epithelial origin tumor and papillary formations (ii) Sarcomatoid mesothelioma, which is similar in appearance to fibrosarcoma and (iii) Biphasic mesothelioma that carries both characteristics of epithelioid and sarcomatoid type (Jeff and Kurt, 2016; Milne *et al.*, 2018). The epithelioid mesothelioma is the most common form in small animals, followed by the sarcomatoid mesothelioma (Carbone *et al.*, 2019; Lajoinie *et al.*, 2022). On the other hand, the biphasic form has only been reported in three dogs and a cat (Sevcikovia *et al.*, 2000; Dias Pereira *et al.*, 2001; Sato *et al.*, 2005; Filho *et al.*, 2015). In human studies, the aggressive behavior of this tumor depends on its type. Epithelioid mesothelioma is the least aggressive one in contrast to sarcomatoid mesothelioma, which is the most aggressive subtype (Carbone *et al.*, 2019; Lajoinie *et al.*, 2022). Nevertheless, biphasic mesotheliomas can behave more or less aggressively depending on the percentage of sarcomatoid components (Carbone *et al.*, 2019). This report describes the macroscopic, histopathologic, and immunohistochemical findings of synchronous tri-cavitary biphasic malignant mesothelioma in a dog with pleural effusions.

Case description

A 7-year-old intact male chihuahua dog was referred to the Prasu Arthorn Animal Hospital, Mahidol University, with respiratory distress as a chief complaint. In a private animal hospital, the physical examination revealed muffled heart sounds, bilaterally dull lung sounds, and hypertension. Bilateral pleural effusion was demonstrated from thoracic radiography. Moreover, the progressive lesion of bone reactions at multiple ribs was found. The neoplasia caused effusion and a bone lesion was suspected. Therefore, the patient was referred for further investigation at this animal hospital. On physical examination, dyspnea with a minimal cough at a respiratory rate of 90 breaths per minute was observed. Cardiopulmonary auscultation revealed muffled heart sounds and bilaterally dull lung sounds. Hematology and blood chemistry profiles were mainly within the normal range, except for severe leukopenia (1,330 cells/µl, reference 6,000 – 17,000 cells/µL). In addition, indirect arterial blood pressure measurement detected hypertension with a systolic blood pressure of 240 mmHg (reference 110 - 160 mmHg). Due to the severe respiratory distress, thoracocentesis was performed to stabilize the patient by intravenously administering fentanyl (2 µg/kg Fentanyl-hameln, Siam Bioscience Co. Ltd., Thailand) and propofol (2 mg/kg Propofol-®Lipuro 1%, B. Braun (Thailand) Ltd., Thailand). Eighty-eight and sixty-two milliliters of cloudy serosanguineous fluid were drained from the left and right hemithorax, respectively. Bacterial and fungal cultures of this fluid were performed. However, neither bacteria nor fungi had grown. The cytology from the pleural fluid revealed a neoplastic effusion that contained numerous, discrete round to oval multinucleated neoplastic cells with basophilic cytoplasm (Fig. 1). Plasmacytoma was differentially diagnosed. The radiographic finding after thoracocentesis showed a periosteal reaction at the sternum and multiple ribs, right lung consolidation, and unclear cardiac silhouette from residue effusion. Echocardiography found neither cardiac abnormalities nor pericardial effusion. Therefore, the following week, a whole-body computerized tomography (CT) scan and biopsy were considered as a further diagnosis plan. The patient was initially stabilized by the control of infection and blood pressure levels, as well as monitoring for respiratory distress to reduce the risk of anesthesia. A combination of marbofloxacin (2.56 mg/kg Marbocyl® P, Vetoquinol, France) and clindamycin (11 mg/kg Antirobe Aquadrop®, Zoetis, Thailand) was orally administered as an antibiotic. An oral dihydropyridine calcium channel blocker with amlodipine (0.16 mg/kg Amlopine, Berlin, Thailand) was prescribed as an antihypertensive agent. However, five days after medical treatment, the patient returned with clinical signs of dyspnea and cyanosis mucous membrane. A second thoracocentesis was performed to drain fluid from both hemithoraces. Unfortunately, the dog died before the appointment for CT scanning and biopsy.

A complete necropsy was performed immediately with the consent of the owner. Patchy red discoloration with multiple white nodules was noted on both sides of the peritoneum when opening the abdominal cavity (Fig. 2D). Approximately 30 milliliters of cloudy red fluid were found inside the abdominal cavity. Fibrin strands were observed in the visceral organs and peritoneum. The thoracic cavity contained 100 milliliters of cloudy serosanguinous fluid in each hemithorax. The lung adhered to the ribcage with fibrin strands. Multiple white to pink nodules were noted at the intercostal muscle, particularly adjacent to

the ribs, after the ribcage was removed (Fig. 2B). An irregular-shaped mass extended from the diaphragm to the pericardium, making them adhere to each other and causing the coalescence of white lesions at the diaphragm (Fig. 2A). A multinodular, irregular-shaped white mass was found at the mediastinum (Fig. 2A). The lungs were generally mottled with dark red discoloration and had a firm consistency (Fig. 2C). The trachea contained a small amount of serous fluid along the way to the bifurcation. The myocardium of the left ventricle was slightly thickened with a visible, moderate to marked degree of nodular endocardiosis of the mitral valve.

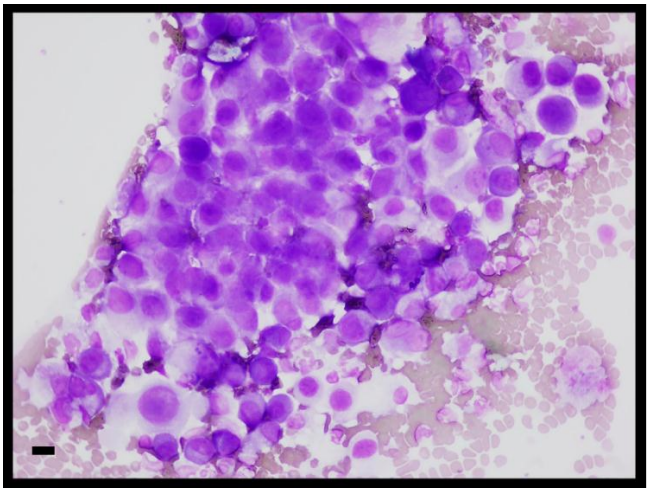

Figure 1 Cytology from a pleural effusion (Diff-Quik staining). Bar = 10 µm.

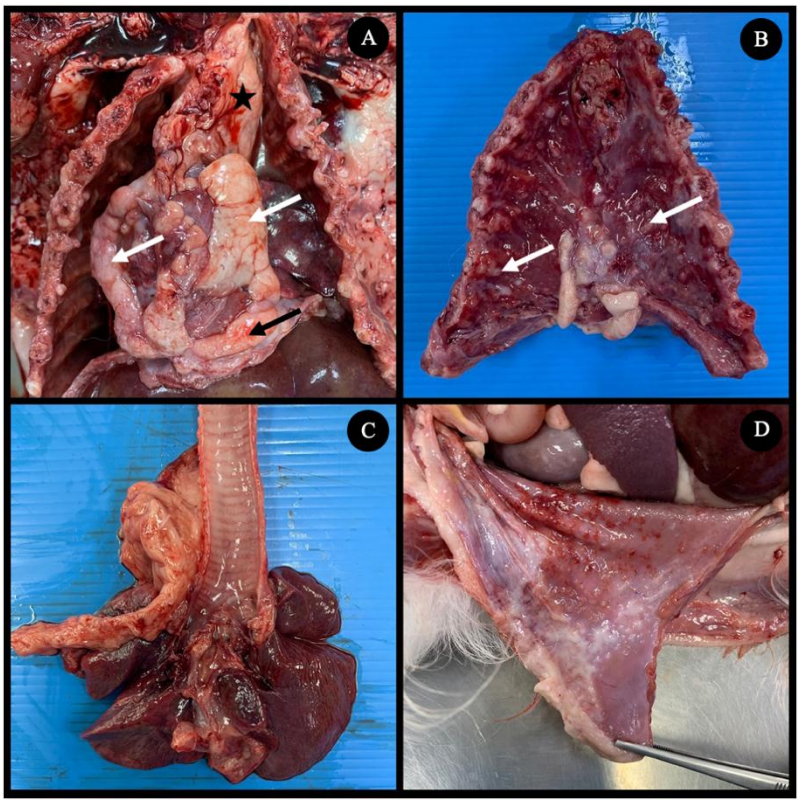

Figure 2 Macroscopic appearances from the necropsy. (A) The irregular-shaped mass extended from the diaphragm (black arrow) to the pericardium (white arrow) and mediastinum (star). (B) Multiple white to pink nodules (white arrow) on the pleural cavity under the ribcage. (C) Lung generally mottled with dark red discoloration and a firm consistency. (D) Patchy red discoloration with multiple white nodules on the peritoneum.

Samples of the lesions, including pericardium, mediastinum, ribs, sternum, lung, and peritoneum, were fixed in 10% buffered formalin, processed for histological examination by routine methods and embedded in a paraffin block. The sections were mounted on glass slides and stained using the hematoxylin and eosin (HE) method. The histopathological analysis indicated the presence of a neoplasm composed of a combination of two distinct cell types: epithelium-like and mesenchymal-like neoplastic cells (Fig. 3). In the pericardium section, there is diffuse thickening of the pericardium, partially

filling it with the nodular structure of neoplastic cells (Fig. 3A). The nodules are mainly composed of neoplastic epithelioid cells mixed with a minor component of spindle-shaped cells (Fig. 3B) with poor, strongly eosinophilic cytoplasm. Neoplastic cells are cuboid, polygonal to spindle-shaped, with variably distinct cell borders, a moderate amount of eosinophilia, often vacuolated cytoplasm, round to ovoid central nuclei, vesicular to stippled chromatin and 1 - 3 nucleoli. There is moderate anisocytosis and anisokaryosis with evidence of nuclear molding. In several regions of the pericardium, nests, and cords of tumor cells extend below the surface and form a less organized proliferation, which is associated with a loose connective tissue stroma containing isolated spindle-shaped cells or large anaplastic cells. Extension of neoplastic cells from the pericardium into the underlying adipose tissue and cardiac muscles is marked. The diaphragm is thickened by infiltrating sheets of neoplastic epithelioid cells and interlacing fascicles of spindle cells. Such neoplastic cells invade and compress the skeletal muscle of the diaphragm. In some areas of the parietal pleura superior to the diaphragmatic surface, there are papillary and micropapillary projections (Fig. 3C), which are supported by fibrovascular stroma covered by one or several layers of pleomorphic mesothelial cells (Fig. 3D). The mediastinum shows diffuse solitary epithelioid cells; none of the sarcomatoid types were observed in this area. In a section of the rib, similar groups of epithelioid neoplastic cells are present on the periosteal surface, within vascular spaces and intramedullary areas (Fig. 3E and 3F). The nodules of the peritoneum are composed of neoplastic epithelioid cells and surrounded by a whorl of spindle cells (Fig. 3G). In the lung parenchyma, a cluster of epithelium-like neoplastic cells was found between interstitial tissue (Fig. 3H), and neoplastic emboli were found in many planes of the slide. A compact polymer detection system was used for immunohistochemistry. The primary antibody MUM-1 (1: 600 Clone MRQ-43; Cell Marque, USA) was used to rule out plasmacytoma from the first differential diagnosis. However, all of the previously mentioned slides demonstrated a negative for MUM-1 (Fig. 4). Furthermore, the primary antibodies vimentin (1: 450 Clone V9; Cell Marque, USA), cytokeratin (1: 1 200 Clone AE1/AE3; Leica Biosystems, United States) and desmin (1: 300 Clone D33; Dako, United States) were used to determine biphasic malignant mesothelioma. The positive to vimentin is used to distinguish epithelioid mesothelioma from vimentin-negative carcinoma tumors. The positive to cytokeratin is used to separate sarcomatous mesothelioma from sarcoma tumor, which is harmful for cytokeratin. The immunoreactivity data in the biphasic mesothelioma are presented in Table 1. The neoplastic cells have a diffuse cytoplasmic expression of both cytokeratin and vimentin. The epithelioid type tends to have intense immunostaining on cytokeratin and weak cytoplasmic expression to vimentin, and vice versa for the sarcomatoid type. Desmin immunostaining presented intense intracytoplasmic regions only in the sarcomatoid type, while the epithelioid are more variable with weak to negative cytoplasmic expression. Immunohistopathologic findings of biphasic mesothelioma are demonstrated in (Fig. 5).

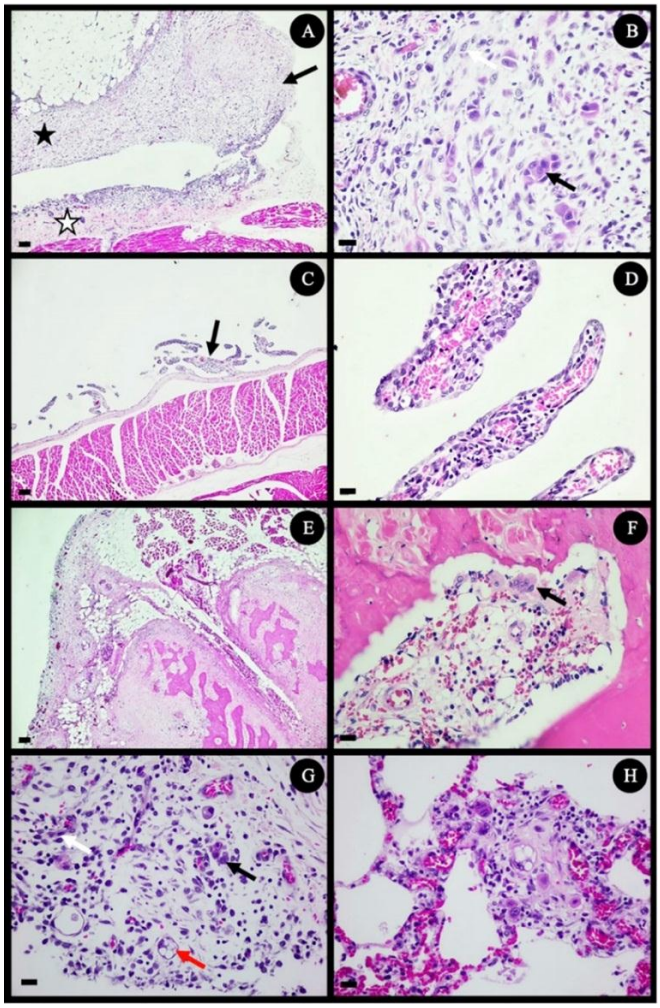

Figure 3 Histological findings of biphasic mesothelioma, HE. (A) Neoplastic nodules (black arrow) at pericardium (black star) and coalescing with diaphragm (white star). Bar = 100 µm. (B) Component of neoplastic epithelioid cells (black arrow) mixed with spindle-shaped cells (white arrow). Bar = 20 µm. (C) Papillary projection at parietal pleura superior to diaphragmatic surface. Bar = 100 µm. (D) High magnification of papillary projection; fibrovascular stroma covered by one or several layers of pleomorphic mesothelial cells. Bar = 20 µm. (E) The rib section has a diffuse neoplastic nodule on the parietal pleura. Bar = 100 µm. (F) The epithelioid neoplastic cells in the intramedullary area. Bar = 20 µm. (G) The cluster of epithelioid neoplastic cells (black arrow) and sarcomatoid neoplastic cells (white arrow) in the peritoneum with vacuolated cytoplasm (red arrow) in some neoplastic cells. Bar = 20 µm. (H) A cluster of neoplastic cells in the lung parenchyma. Bar = 20 µm.

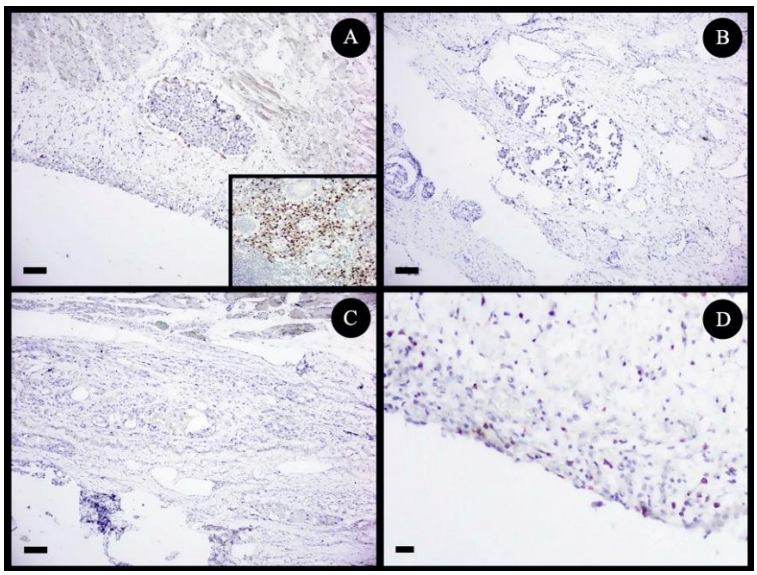

Figure 4 Negative immunostaining of MUM-1 in epithelioid neoplastic cells on the diaphragm (A), the pericardium (B), and the rib (C). Bar = 100 µm. (D) Negative immunostaining of MUM-1 in sarcomatoid neoplastic cells on the parietal pleura. Bar = 20 µm. The positive controls of MUM-1 are shown as an inset in the lower right corner.

Table 1 Immunochemistry details of biphasic mesothelioma in this case

Location	Cell type	Cytokeratin	Vimentin	Desmin
Pericardium	Epithelioid	(++)	(++)	(+)
	Sarcomatoid	(+)	(++)	(++)
Parietal pleura	Epithelioid	(++)	(+)	(-)
	Sarcomatoid	(+)	(++)	(++)
Diaphragm	Epithelioid	(++)	(+)	(-)
	Sarcomatoid	(+)	(++)	(++)
Peritoneum	Epithelioid	N/A	(++)	N/A
	Sarcomatoid	N/A	(++)	N/A
Mediastinum	Epithelioid	(+)	(++)	N/A
Rib	Epithelioid	(++)	(+)	(-)
Lung	Epithelioid	N/A	(++)	N/A

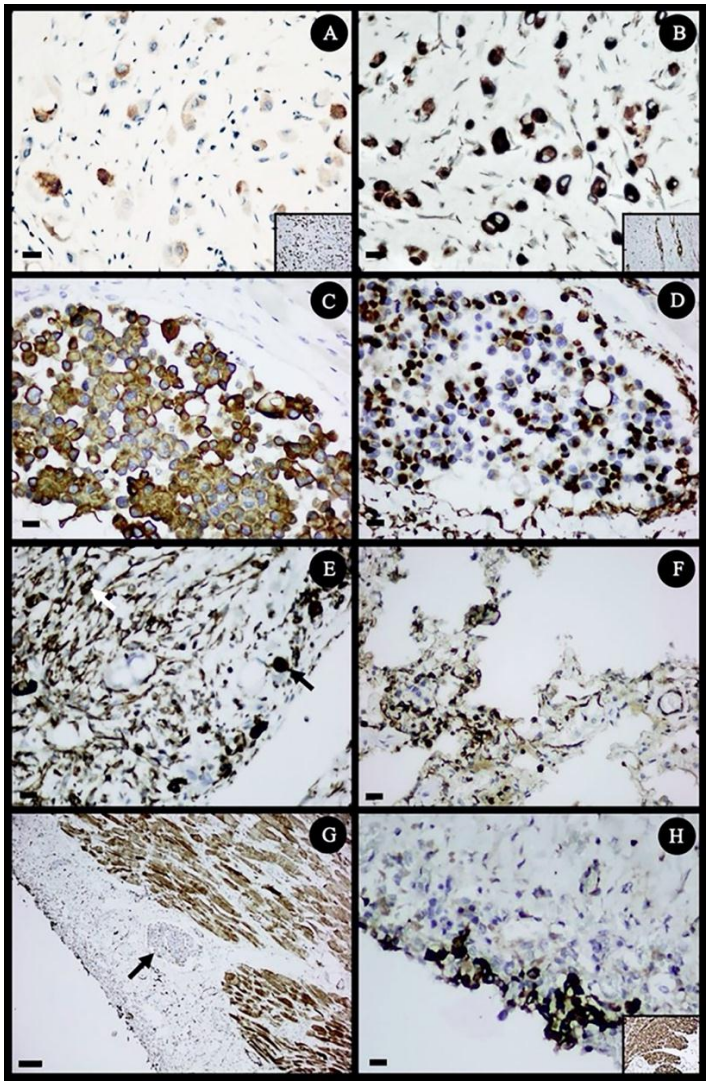

Figure 5 Immunohistopathologic findings of biphasic malignant mesothelioma. (A) Weak immunostaining of cytokeratin in epithelioid neoplastic cells on the mediastinum. Bar = 20 µm. (B) Intense immunostaining of vimentin in epithelioid neoplastic cells on the mediastinum. Bar = 20 µm. (C) Intense immunostaining of cytokeratin in epithelioid neoplastic cells on the pericardium. Bar = 20 µm. (D) Diffuse intense immunostaining of vimentin in epithelioid neoplastic cells on the pericardium. Bar = 20 µm. (E) Intense immunostaining of vimentin in epithelioid neoplastic cells (black arrow) and sarcomatoid neoplastic cells (white arrow) on the peritoneum. Bar = 20 µm. (F) Intense immunostaining of vimentin in epithelioid neoplastic cells on lung parenchyma. Bar = 20 µm. (G) Absence of immunostaining of desmin in epithelioid neoplastic cells (black arrow) on the diaphragm. Bar = 100 µm. (H) Intense immunostaining of desmin in sarcomatoid neoplastic cells on the parietal pleura. Bar = 20 µm. The positive controls of cytokeratin (A), vimentin (B), and desmin (H) are shown as an inset in the lower right corner.

Discussion

Mesothelioma can be differentiated into epithelioid, sarcomatoid, or biphasic types (Jeff and Kurt, 2016). Histologically, this case demonstrated the biphasic morphology of mesothelioma, which consists of a combination of mainly epithelioid and minor sarcomatoid components. Biphasic mesothelioma is scarce in small animal medicine, with a single case

documented in a cat and three cases in dogs (Sevcikovia *et al.*, 2000; Dias Pereira *et al.*, 2001; Sato *et al.*, 2005; Filho *et al.*, 2015). The affected location in all three dogs was the peritoneum, whereas a cat was affected in the pericardium and pleura, acting as a bi-cavitary mesothelioma. To the authors' knowledge, this is the first report of a biphasic tri-cavitary mesothelioma in this species. Regarding the presentation age, this case was similar to the previous report that mesothelioma is typically reported at the age of 3 to 13 years old, with an average age of over eight years, and most of them were pure large-breed dogs (Kapakain *et al.*, 2012; Lajoinie *et al.*, 2022). The breed that was most frequently noticed was the Golden Retriever, with the German Shepherd, Yorkshire Terrier, Bernese Mountain Dog, and American Staffordshire Terrier following closely behind in the representation (Lajoinie *et al.*, 2022), while the Chihuahua, which is a small-breed dog, is reported in this case. The exact etiological factors for the cause of mesothelioma are still poorly understood. One of the factors has evidence of association with asbestos and silica exposure (Lawrence *et al.*, 1983). The presence of residual pulmonary asbestos has been observed in nearly everyone in the general population. Urban dwellers are more prone to a greater prevalence of lung asbestosis than rural residents (Becklake, 1982). Furthermore, a research investigation on dogs living in urban areas revealed that 83.3% of the subjects exhibited the presence of asbestos in their pulmonary tissue (Harbison and Godleski, 1983). These dogs lived in an urban environment, similar to the present case. Therefore, it may be noticed that this dog's living conditions may be a risk factor for mesothelioma. However, no assessment was performed to determine the presence of asbestos in the lung tissue in this case.

In this case, the gross appearance and locations of the tumor as determined by necropsy and the microscopic findings of histopathology and immunohistochemistry are consistent with a mesothelioma diagnosis. Mesothelioma is typically a low-grade local malignancy tumor, while metastasis is rarely reported (Head *et al.*, 2002). This tumor commonly affects only one or two of these three locations, including the pleura, pericardium, and peritoneum (Lajoinie *et al.*, 2022). Interestingly, in this case, the involvement of all locations is an unusual distribution for this tumor. The presence of multifocal patterns and neoplastic emboli suggests the tumor spread by a hematogenous route. However, the primary location of the lesion is still unknown. The diagnosis was confirmed with cytokeratin, vimentin, and desmin immunohistochemical staining in this case. The cells resembling epithelium showed the expression of both vimentin and cytokeratin, whereas the sarcomatoid constituents demonstrated a solid response to vimentin but a weak positive reaction to cytokeratin. The simultaneous expression of vimentin and cytokeratin has been identified as a histological type of mesothelioma (Milne *et al.*, 2018). In this case, the intense positive to desmin staining was observed, particularly in sarcomatoid mesothelioma, while epithelioids are more variable with weak to negative cytoplasmic expression. In contrast to a study using immunocytochemistry staining to diagnose serosal neoplasm in dogs, mesenchymal origin cells, including normal mesothelial cells, reactive mesothelial, and mesothelioma, tend to have strong immunostaining of cytokeratin, vimentin and desmin (Przeździecki and Sapierzyński, 2014). However, desmin immunostaining could not be performed on all of the samples in this case due to the limitations of diagnosis costs with the IHC technique. We cannot confirm the variation in cytoplasmic expression of desmin in other regions. Based on the identification of two distinct histological cell types of mesothelioma with the confirmation from cytokeratin and vimentin expression in all three locations, including the pleura, pericardium, and peritoneum, the tri-cavitary biphasic mesothelioma was the tentative diagnosis in this case.

Management of mesothelioma cases constitutes a significant challenge, particularly in the case of thoracic mesothelioma with severe pleural effusion that can affect respiratory function through restrictive ventilation, reduced chest wall expansion, and a decrease in lung volume (Filho *et al.*, 2015). In this case, the cause of death was probably pleural effusion, considering the rapid re-accumulation of thoracic fluid. The development of pleural effusion may result from the tumor itself or obstruction of neoplastic emboli, which causes an increase in oncotic pressure and extravascular leakage (Laura, 2020). Another handling challenge in mesothelioma cases is the difficulty of achieving an early diagnosis. Definitive identification of these neoplasms occurs after the animal is in a critical stage or after mortality (Stepien *et al.*, 2000; Ceribasi *et al.*, 2013). Non-invasive methods such as cytology often offer inconclusive results or misdiagnoses of other tumors (Stepien *et al.*, 2000; Laura, 2020). Likewise, plasmacytoma was incorrectly identified based on the fluid cytology of the effusion in this case. In addition to the complicated diagnostic procedure, tumor therapy is challenging. Mesothelioma in humans often affects the pleura. Surgical excisions and platinum-based chemotherapy treatment, such as cisplatin or carboplatin, are advised when this occurs (Janes *et al.*, 2021; Nadal *et al.*, 2021). In some cases, surgical resection has been described to decrease the effusion or cytoreduction before chemotherapeutic treatment (Atencia *et al.*, 2013; Michelotti *et al.*, 2019). For chemotherapy, the recent report shows intravenous or intracavitary carboplatin use to treat canine mesothelioma. Although chemotherapy-treated dogs had longer median survival times than non-treated dogs, the overall response rate is relatively low (Moberg *et al.*, 2022). Therefore, canine mesothelioma has a poor prognosis for the aforementioned reasons.

In conclusion, the current report presents a case of a synchronous tri-cavitary biphasic malignant mesothelioma in a Chihuahua dog that presented with dyspnea. Interestingly, the effective diagnostic approach for canine malignant mesothelioma should be investigated in further studies.

References

Atencia S, Doyle RS and Whitley NT 2013. Thoracoscopic pericardial window

for management of pericardial effusion in 15 dogs. J Small Anim Pract. 54(11): 564-569.

Becklake MR 1982. Asbestos-related diseases of the lungs and pleura: current clinical issues. Am Rev Respir Dis. 126(2): 187-194.

Carbone M, Adusumilli PS, Alexander HR, Baas P, Bardelli F, Bononi A, Bueno R, Felley-Bosco E, Galateau-Salle F, Jablons D, Mansfield AS, Minaai M, de Perrot M, Pesavento P, Rusch V, Severson DT, Taioli E, Tsao A, Woodard G, Yang H, Zauderer MG and Pass HI 2019. Mesothelioma: Scientific clues for prevention, diagnosis, and therapy. CA Cancer J Clin. 69(5): 402-429.

Ceribasi S, Ozkaraca M, Ceribasi AO and Ozer H 2013. Pericardial Mesothelioma in a German Shepherd Dog: a case report. Vet Med (Praha). 58: 594-598.

Cobb MA and Brownlie SE 1992. Intrapericardial neoplasia in 14 dogs. J Small Anim Pract. 33(7): 309-316.

Dias Pereira P, Azevedo M and Gärtner F 2001. Case of malignant biphasic mesothelioma in a dog. Vet Rec. 149(22): 680-681.

Filho SJ, Magalhães G, Conforti V, Santilli J and Calazans S 2015. Biphasic pericardial and pleural mesothelioma in a cat: A case report. Vet Med (Praha). 60: 105-108.

Francisco AU, Brandon LP and Jesse MH 2016. Jubb, Kennedy & Palmer's Pathology of Domestic Animals. 6th ed. St. Louis: Elsevier. 256.

Harbison ML and Godleski JJ 1983. Malignant mesothelioma in urban dogs. Vet Pathol. 20(5): 531-540.

Head K, Else R and Dubielzig R 2002. Tumors of serosal surfaces. In: Tumors in Domestic Animals. 4th ed. DJ Meuten (ed). Ames: Iowa State Press. 477-478.

Janes SM, Alrifai D and Fennell DA 2021. Perspectives on the Treatment of Malignant Pleural Mesothelioma. N Engl J Med. 385(13): 1207-1218.

Jeff LC and Kurt JW 2016. Respiratory System. In: Jubb, Kennedy & Palmer's Pathology of Domestic Animals. 6th ed. MG Maxie (ed). St. Louis: Elsevier. 523.

Kapakain KAT, Haziroglu R, Gursan N and Yucel G 2012. Mesothelioma in a dog. Ankara Univ Vet Fak Derg. 59: 151-153.

Lajoinie M, Chavalle T, Floch F, Sayag D, Lanore D, Ponce F and Chamel G 2022. Outcome of dogs treated with chemotherapy for mesothelioma: A retrospective clinical study on 40 cases and a literature review. Vet Comp Oncol. 20(4): 825-835.

Laura DG 2020. Mesothelioma. In: Withrow & MacEwen's Small Animal Clinical Oncology. 6th ed. DM Vail and SJ Withrow (eds). St. Louis: Elsevier. 784.

Lawrence TG, Linda MD, Tobi GM, Richard RD and Andrew C 1983. Mesothelioma in pet dogs associated with exposure of their owners to asbestos. Environ Res. 32(3): 305-313.

Michelotti KP, Youk A, Payne JT and Anderson J 2019. Outcomes of dogs with recurrent idiopathic pericardial effusion treated with a 3-port right-sided thoracoscopic subtotal pericardiectomy. Vet Surg. 48(6): 1032-1041.

Milne E, Martinez Pereira Y, Muir C, Scase T, Shaw DJ, McGregor G, Oldroyd L, Scurrell E, Martin M, Devine C and Hodgkiss-Geere H 2018. Immunohistochemical differentiation of reactive from malignant mesothelium as a diagnostic aid in canine pericardial disease. J Small Anim Pract. 59(5): 261-271.

Moberg HL, Gramer I, Schofield I, Blackwood L, Killick D, Priestnall SL and Guillén A 2022. Clinical presentation, treatment and outcome of canine malignant mesothelioma: A retrospective study of 34 cases. Vet Comp Oncol. 20(1): 304-312.

Nadal E, Bosch-Barrera J, Cedrés S, Coves J, García-Campelo R, Guirado M, López-Castro R, Ortega AL, Vicente D and de Castro-Carpeño J 2021. SEOM clinical guidelines for the treatment of malignant pleural mesothelioma (2020). Clin Transl Oncol. 23(5): 980-987.

Przeździecki R and Sapierzyński R 2014. Using of immunocytochemistry in differential diagnosis of neoplasms of serosal cavities in dogs. Pol J Vet Sci. 17(1): 149-159.

Sato T, Miyoshi T, Shibuya H, Fujikura J, Koie H and Miyazaki Y 2005. Peritoneal Biphasic Mesothelioma in a Dog. J Vet Med. 52(1): 22-25.

Sevcikovia Z, Kolodzieyski L, Levkut M, Ledecky V and Sevcik A 2000. Malignant biphasic peritoneal mesothelioma in a dog. Indian Vet J. 77: 852-855.

Smith DA and Hill FW 1989. Metastatic malignant mesothelioma in a dog. J Comp Pathol. 100(1): 97-101.

Stepien RL, Whitley NT and Dubielzig RR 2000. Idiopathic or mesothelioma-related pericardial effusion: clinical findings and survival in 17 dogs studied retrospectively. J Small Anim Pract. 41(8): 342-347.